12-13-2002

Accuracy Study of a Free Particle Using Quantum Trajectory Method on Message Passing Architecture

Ravi K. Vadapalli

ACCURACY STUDY OF A FREE PARTICLE USING QUANTUM TRAJECTORY METHOD ON MESSAGE PASSING ARCHITECTURE

By

Ravi K. Vadapalli

A Thesis
Submitted to the Faculty of
Mississippi State University
in Partial Fulfillment of the Requirements
for the Degree of Master of Science
in Computational Engineering
in the College of Engineering

Mississippi State, Mississippi

December 2002

ACCURACY STUDY OF A FREE PARTICLE USING QUANTUM TRAJECTORY METHOD ON MESSAGE PASSING ARCHITECTURE

By

Ravi K. Vadapalli

Approved:

Anthony Skjellum Associate Professor of Computer Science (Major Advisor)	David H. Huddleston Associate Professor of Civil Engineering (Committee Member)
Seth F. Oppenheimer Associate Professor of Mathematics (Committee Member)	
Boyd Gatlin Associate Professor of Aerospace Engineering & Graduate Coordinator	A. Wayne Bennett Dean of the College of Engineering

Name: Ravi K. Vadapalli

Date of Degree: December 13, 2002

Institution: Mississippi State University

Major Field: Computational Engineering

Major Professor: Dr. Anthony Skjellum

Title of Study: ACCURACY STUDY OF A FREE PARTICLE USING QUANTUM TRAJECTORY METHOD ON MESSAGE PASSING ARCHITECTURE

Pages in Study: 41

Candidate for Degree of Master of Science

Bohm's hydrodynamic formulation (or quantum fluid dynamics) is an attractive approach since, it connects both classical and quantum mechanical theories of matter through Hamilton-Jacobi (HJ) theory, and quantum potential. Lopreore and Wyatt derived and implemented one-dimensional quantum trajectory method (QTM), a new wave-packet approach, for solving hydrodynamic equations of motion on serial computing environment. Brook et al. parallelized the QTM on shared memory computing environment using a partially implicit method, and conducted accuracy study of a free particle. These studies exhibited a strange behavior of the relative error for the probability density referred to as the *transient effect*.

In the present work, numerical experiments of Brook et al. were repeated with a view to identify the physical origin of the *transient effect* and its resolution. The

present work used the QTM implemented on a distributed memory computing environment using MPI. The simulation is guided by an explicit scheme.

DEDICATION

To the holy feet of shree sai baba and to Sarada, my dear wife, for her love, understanding, and constant companionship.

ACKNOWLEDGMENTS

I am gratefully indebted to my thesis advisor Dr. Anthony Skjellum for his able guidance, and funding with out which, I could not have completed this program. I am very thankful to my committee members Dr. David H. Huddleston, and Dr. Seth F. Oppenheimer for their interest in this work and for their advise.

I take this opportunity to record my thanks to Dr. Ioana Banicescu for funding part of this research activity and for all her support in this endeavor. I must thank Mr. Glenn Brook for the OpenMP code, and Dr. Cariño for his collaboration in implementation of the MPI version of the code, and Dr. Paul Oppenheimer for his feedback.

I also would like to thank Dr. Bradly Carter, and Dr. David Marcum for providing computational facilities and excellent work environment. Additional thanks to my colleagues at the High Performance Computing Laboratory, for their help and friendship. I am very thankful to Dr. Raghu Machiraju for his timely advise and help in switching my interests into Computational Engineering.

Deepest thanks go to my mother, and brothers for all the encouragement they have provided and the faith they have shown in me.

TABLE OF CONTENTS

CHAPTER Page

LIST OF FIGURES

NOMENCLATURE

p	Momentum
m	Mass
E	Energy
N	Number of pseudoparticles
β	Width of the wave-packet
k	Wave vector
k_0	initial wave vector
ρ	Probability density
v_0	Initial velocity
Q	Quantum Potential
f_q	Quantum Force
V	Classical Potential
f_c	Classical Force
R	Amplitude function
S	Phase function
t	Time
ω	Frequency of plane wave
Δt	timestep size
Δx	spatial resolution
$\hat{H}$	Hamiltonian opeartor
$\hat{p}$	Momentum operator
$\hbar$	Planck's Constant divided by 2π

CHAPTER I

INTRODUCTION

The quantum world is inexplicable in classical terms. Predictions of Newtonian mechanics fail in quantum mechanical regimes particularly because of the apparent indeterminism associated with quantum mechanics. This means, that individual atomic events are unpredictable, uncontrollable, and literally seem to have no cause. Regularities in these systems emerge only when one considers a large ensemble of such events. This indeed is generally considered as conceptual problem with quantum mechanics, necessitating a fundamental revision of deterministic classical theory. Some of the principal phenomena of interest in quantum mechanics are interference, tunneling [1] and nonlocal correlations[2]. All these phenomena with fundamentally discrete, statistical, and nonlocal character, and clearly conflict with continuous, deterministic, and generally local structure of classical mechanics. Thus, the challenge now is to develop a theory of individual material systems such that, their mean behavior corresponds to the predictions of the statistical (or nondeterministic) behavior of quantum mechanics.

Time-dependent Schrödinger equation (TDSE)

$$i\hbar\frac{\partial\Psi}{\partial t} = \hat{H}\Psi, \qquad \hat{H} \equiv -\frac{\hbar^2}{2m}\nabla^2 + V, \tag{1.1}$$

offers the mathematical model for quantum dynamics. TDSE represents the governing equation of a quantum mechanical system composed of a single particle of mass m moving in a potential V, and $\hat{H}$ is the Hamiltonian operator which is a

sum of the kinetic energy operator and the interaction potential V. The solution of the TDSE represents the system wavefunction $\Psi(\vec{r}, t)$ that inherits the statistical nature of the quantum mechanics.

Since there is no way to describe individual processes using just the wavefunction, de Broglie [3, 4, 5] proposed that the wavefunction be associated with an ensemble of identical particles differing in their positions and distributed in space such that the total probability density $|\Psi|^2 = 1$. Thus, the wavefunction not only determines the likely location of a particle but also acts as a 'pilot-wave' that guides the particle (only one of which accompanies each wave), into regions where Ψ is most intense.

With a view to introducing the particle concept into quantum mechanics, Madelung [6, 5] expressed the wavefunction in polar form

$$\Psi(\vec{r}, t) = R(\vec{r}, t)e^{iS(\vec{r},t)/\hbar} \tag{1.2}$$

where, R is the real-valued amplitude function and S is the real-valued phase function. This interpretation yields information on the overall structure of a wave as a single physical entity propagating in space. Since this interpretation is analogous to a wave-packet (see next section) whose amplitude is appreciable only in a limited region, they are widely used to study atomic, molecular, chemical, and condensed matter physics. The time-dependent wave-packet methods have several advantages. Their computational analysis is closely related to experimental laboratory methods. Since the wavefunction represented by time-dependent wave-packet is normalizable and is defined in the standard Hilbert space, these methods are popular in scattering theory (see [7] for example).

1.1 Wave Packet Method

It is reasonable to suppose that a free particle of momentum **p** is associated with a harmonic plane wave of vector **k** such that **p**=$\hbar$**k**. Further E, the energy of a classical particle, has its quantum analogue defined by E=$\hbar\omega$ where, ω is the frequency of the wave. To represent a physical particle (confined to a region in space), with a plane wave(that could spread upto infinity), several plane waves (also called wavefunction, solution of the TDSE (Eqn. 1.1) could be superposed and by arranging their amplitudes and phases so that they constructively interfere in a restricted region of space, and destructively interfere outside this region. By exploiting the analogies of particle and wave properties of matter, and to ascertain physical properties represented by a plane wave, let us assume that only a finite range of **k** values contribute to the physical properties. Such an approximation is known as wave-packet approximation. According to the correspondence principle, such a wave-packet centered around the coordinate origin (k_0), must describe classically the motion of a free particle.

Using the classical relationship E=$p^2/2m$ and using the above definitions for **p** and E, we get

$$\omega = \frac{\hbar^2\mathbf{k}^2}{2m} \tag{1.3}$$

In the above ω−k relationship, $\hbar^2$/2m is the rate of spreading (relative separation of the trajectories with time) of the wave-packet. Typical spreading of a wave-packet with QTM is shown in Fig. 1.1. Considering one-dimensional case for which k_x=k, and k_y=k_z=0, the motion of the wave-packet, that represents a moving free particle in one-dimension, can be approximated by expanding $\omega(k)$ around k_0 to get

$$\omega(k) = \omega(k_0) + \frac{d\omega}{dk}(k-k_0) + \frac{d^2\omega}{dk^2}(k-k_0)^2 + \cdots \tag{1.4}$$

If $|k - k_0|$ is sufficiently small then, the contribution of the quadratic term could be safely ignored with out loss of generality. Then, the above equation is reduced to

$$\omega(k) = \omega(k_0) + \frac{d\omega}{dk}(k - k_0) \tag{1.5}$$

Physically this means that, a wave-packet formed by superposing a finite set of plane waves, each with a different k, centered around some k_0 accurately represents a particle. In the above equation (Eqn. 1.5), $v_g = \frac{d\omega}{dk}$, with dimensions of velocity, is called the group (average) velocity of the wave-packet. Thus, v_g corresponds to the particle velocity.

1.2 Quantum Fluid Dynamics

Bohm [8, 9] extended the particle concept in quantum mechanics to establish a relationship between two physical theories of matter: classical mechanics and quantum mechanics to describe the spacetime picture of quantum mechanics. Although there are several approaches, such as expressing classical mechanics in Hilbert space [5], introducing a kind of phase space to quantum mechanics through Wigner functions [10], Bohm associated a well-defined phase space (simultaneously with real position, and momentum) with the quantum mechanical processes in spacetime. By treating both classical and quantum mechanical phenomena as particular instances of a suitably generalized Hamilton-Jacobi (HJ) theory, Bohm developed a hydrodynamic formulation in quantum mechanics, also called quantum fluid dynamics (QFD), analogous to computational fluid dynamics (CFD). With generalized HJ theory providing a mathematical procedure for how one passes from the quantum to the classical domain, Bohm derived a formalism that connects classical and quantum mechanical pictures through Q, the quantum potential. In the QFD approach, the fluid is characterized by ρ, the density of a compressible

and irrotational fluid and, v the velocity field of the fluid, and m is the mass of a particle traveling in the fluid. With the QFD formulation since R and S are nearly monotonic functions of time, this formulation is computationally advantageous for parallel processing.

With close parallelism between CFD and QFD, and with demonstrated success of CFD for classical domain [11], it would be interesting to explore the applicability of CFD techniques in QFD. With this insight, Lopreore and Wyatt [12] developed and implemented the quantum trajectory method (QTM). This is a new wave-packet method derived from the QFD approach for solving the QFD-equations of motion (QFD-EOM) [12]. In this method, the derivatives of the field vectors namely, ρ, v, and Q are computed using the moving least squares (MLS) algorithm [12]. Further details of the QTM and MLS methods will be discussed in Chapter 2.

The present application of the QTM is to compute the solution of the TDSE (Eqn. 1.1). In order to simplify the implementation of the method all quantities are expressed in atomic units (a.u.) ($\hbar$=m_e=e=1) where, $\hbar$ is Planck's constant divided by 2π, m_e is the mass of the electron, and e is its charge. Though $\hat{H}$, the Hamiltonian operator, explicitly depends on time through an interaction potential, for current applications, $\hat{H}$ is assumed to be time-independent.

1.3 Previous Studies

Lopreore and Wyatt [12] derived and implemented one-dimensional QTM using an MLS algorithm on a serial computing environment. Brook et al. [13] parallelized the MLS algorithm for shared-memory model using OpenMP directives. They employed a partially implicit method for updating the density and velocity fields and an explicit method for remaining component vectors. They also conducted

accuracy study of the probability density of a free particle moving with a velocity v_0. In their study, they used a Gaussian wave-packet (GWP) to represent the initial wavefunction. With the density field initialized directly from the GWP, their accuracy study exhibited a strange behavior in relative error during 0-125 a.u. of propagation of the wave-packet. For the remainder of the discussion, this behavior is referred to as the *transient effect*. This effect, at the outset, contradicts a nearly monotonic behavior of density with the QFD formalism [8, 9]. Brook et al. [13] also observed that, the amplitude of the *transient effect* is more sensitive to the size of the time step (Δt) compared to the spatial resolution (Δx). Their results (reproduced in the present work) are shown in Figs. 1.2 and 1.3.

1.4 Transient Effect

From Fig. 1.3, it is clear that the amplitude of the *transient effect* is decreasing with decreasing Δt. This could mean that the *transient effect* is due to the numerical inaccuracies and discretization errors. If the *transient effect* were due to the discretization errors it should vanish completely for sufficiently small Δt. With such a choice, it is also expected to reproduce the trends in relative error in conformity with the expected nearly monotonic behavior in density with the QFD formalism.

With this view, numerical experiments of Brook et al. [13] were repeated using Δt=0.001 and N=21. The relative error is as shown in Fig. 1.4. From this figure, though the relative error is very small, the relative amplitude of the *transient effect* with respect to the maximum error is more or less independent of Δt. This means, the strange behavior of the relative error remains regardless of the size of the time step. Thus, it is clear that the *transient effect* has a physical origin apart from numerical inaccuracies.

1.5 Present Study

Shared-memory parallel computers are not as widely popular as the distributed memory computing environments. Since large scale computational simulation is efficient and cost effective on a distributed computing environment particularly with the availability of architecture independent Message Passing Interface (MPI) communication libraries, the presented study employed the MPI version of the QTM.

With distributed computing environment, since the partially implicit scheme contributes more to the communication overhead than to the accuracy (at least for the present study), a fully explicit scheme is employed for propagating the wave-packet in the current investigation. The present work validated the MPI implementation of the QTM by conducting the accuracy study of a free particle.

Since Q depends on the curvature of the density rather than its amplitude [12], onset of the *transient effect* for probability density transforms into similar behavior in the relative error for Q. Since quantum mechanics is abstracted through Q in the QFD formalism, its accurate representation is vital for appropriate simulation of quantum dynamics. Identification of the physical origin of the *transient effect* and its resolution thus, formed the motivation of the present work.

The remainder of the thesis is organized as follows. Chapter 2 provides a synopsis of the QFD-EOM, MLS algorithm, and the QTM. Chapter 3 details on the fully explicit algorithm and its implementation on MPI. Chapter 4 introduces a new method for removing the anomalies due to the *transient effect*. Results and discussions are provided in Chapter 5 followed by summary and conclusions, and the future work in Chapter 6.

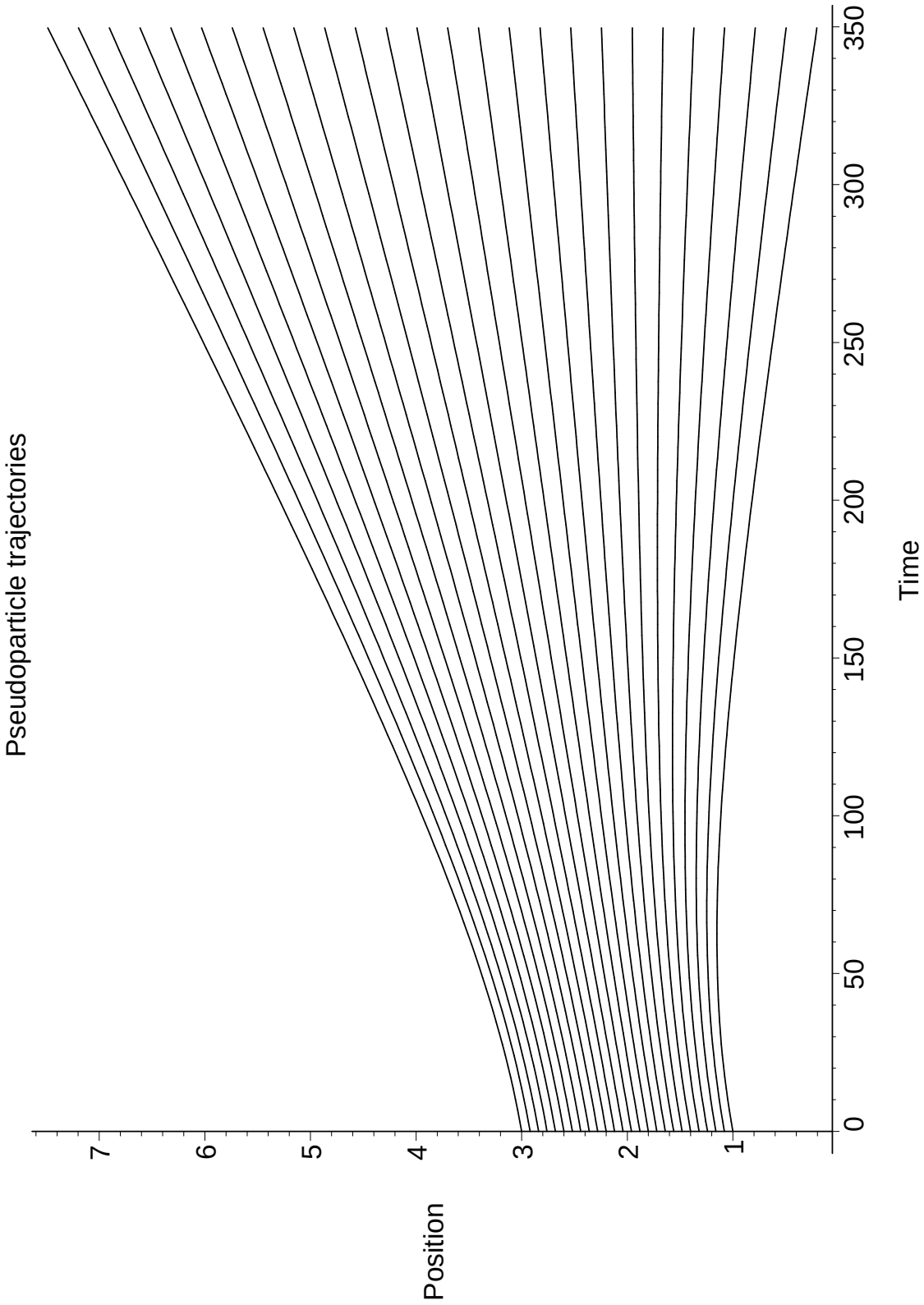

Figure 1.1: Spreading of a moving free particle wave-packet

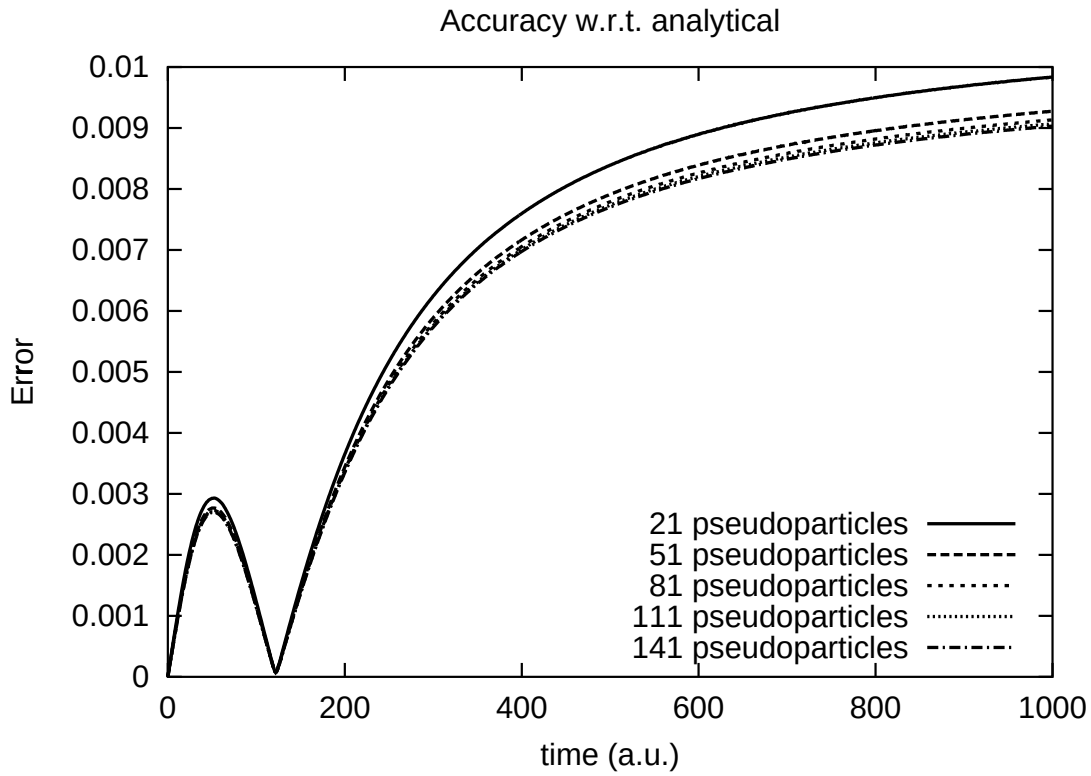

Figure 1.2: Dependence of accuracy of probability density on Δx when $\Delta t = 0.1$

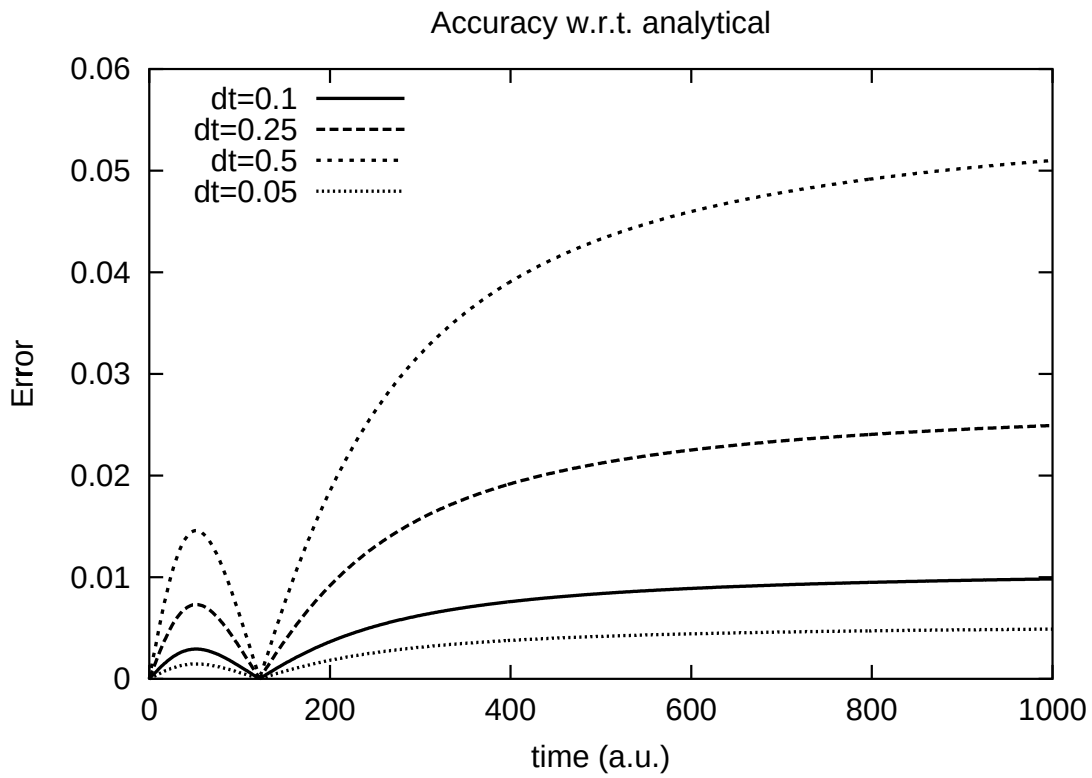

Figure 1.3: Dependence of accuracy of probability density on Δt when $\Delta x = 0.095$

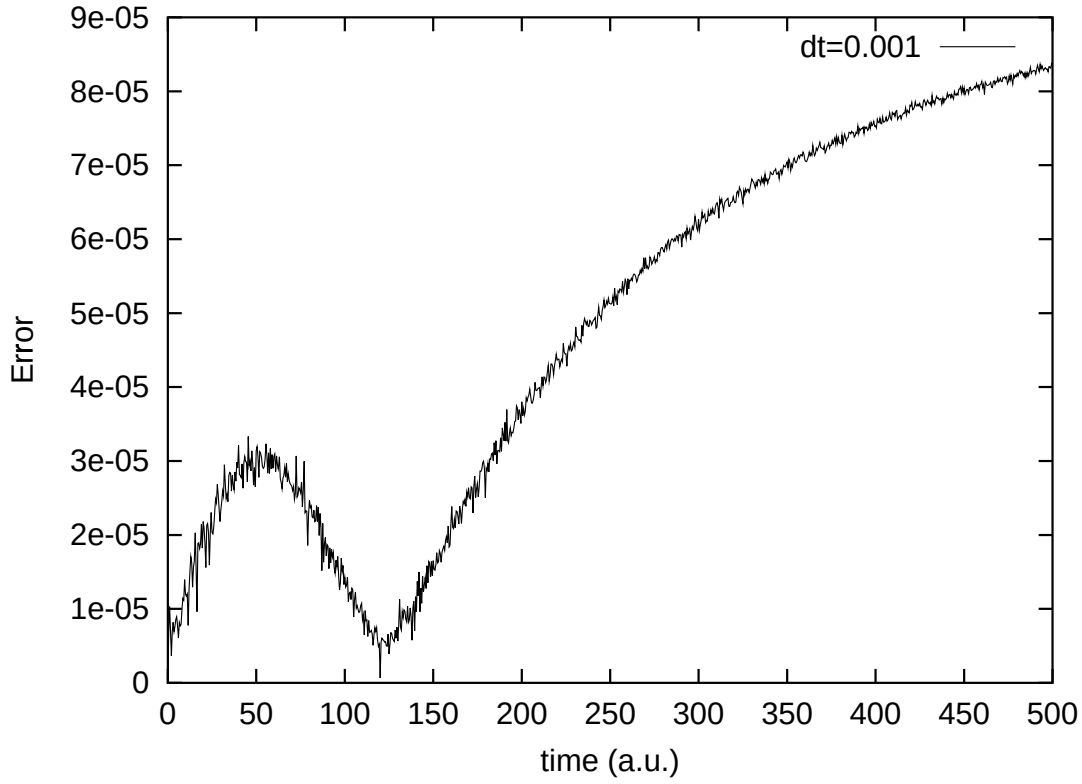

Figure 1.4: Transient Effect for Δt=0.001 and Δx=0.095

CHAPTER II

BACKGROUND

2.1 Governing Equations

The first step in deriving the QFD-EOM is to choose between the Eulerian formulation [14, 15, 16] and Lagrangian formulation [17]. The present study used Lagrangian formulation in view of its advantages. The Lagrangian equations resemble Newton's second law and the continuity equation [12, 18]. In Lagrangian formulation, the computation is focused onto "regions of highest probability as an optimal adaptive grid" [18]. Also, the Lagrangian formulation is advantageous for formulating problems for parallel processing.

The next step is to substitute the wavefunction in polar form

$$\Psi(\vec{r},t) = R(\vec{r},t)e^{iS(\vec{r},t)/\hbar} \tag{2.1}$$

into the TDSE.

$$i\hbar\frac{\partial\Psi}{\partial t} = \hat{H}\Psi, \qquad \hat{H} \equiv -\frac{\hbar^2}{2m}\nabla^2 + V, \tag{2.2}$$

Separating into real and imaginary parts and defining

$$\rho(\vec{r},t) = R^2(\vec{r},t) \qquad \text{probability density,} \tag{2.3}$$

$$v(\vec{r},t) = \frac{1}{m}\nabla S(\vec{r},t) \qquad \text{velocity and,} \tag{2.4}$$

$$j(\vec{r},t) = \rho(\vec{r},t)v(\vec{r},t) \qquad \text{flux} \tag{2.5}$$

we get the Euler QFD-EOM:

$$-\frac{\partial \rho(\vec{r},t)}{\partial t} = \vec{\nabla}\cdot\left[\rho(\vec{r},t)\frac{1}{m}\vec{\nabla}S(\vec{r},t)\right], \tag{2.6}$$

$$-\frac{\partial S(\vec{r},t)}{\partial t} = \frac{1}{2m}\left[\vec{\nabla}S(\vec{r},t)\right]^2 + V(\vec{r},t) + Q(\rho;\vec{r},t), \tag{2.7}$$

(Eqn. 2.7) is the *quantum Hamilton-Jacobi* (HJ) equation. This is identically in the form of classical HJ equation except for the last term Q, the quantum potential which is inherently global in nature. Q is defined as follows:

$$\begin{aligned} Q(\rho;\vec{r},t) &= -\frac{1}{2m}\frac{1}{R}\nabla^2 R = -\frac{1}{2m}\frac{1}{\rho^{1/2}}\nabla^2\rho^{1/2} \\ &= -\frac{1}{2m}(\nabla^2\log\rho^{1/2} + |\nabla\log\rho^{1/2}|^2). \end{aligned} \tag{2.8}$$

Taking the gradient of (Eqn. 2.7) the velocity update is derived as follows:

$$m\frac{d\vec{v}}{dt} = -\vec{\nabla}(V+Q) = \vec{f_c} + \vec{f_q}, \tag{2.9}$$

where, $\vec{f_c} \equiv -\vec{\nabla}V$ (the classical force term) and $\vec{f_q} \equiv -\vec{\nabla}Q$ (quantum force term). Applying the Lagrangian time derivative

$$\frac{d}{dt} = \frac{\partial}{\partial t} + \vec{v}\cdot\vec{\nabla} \tag{2.10}$$

to (Eqn. 2.6) one obtains

$$\left[\frac{\partial}{\partial t} + \vec{v}\cdot\vec{\nabla}\right]\rho = \frac{d\rho}{dt} = -\rho\vec{\nabla}\cdot\vec{v}, \tag{2.11}$$

which on integrating produces the density update equation

$$\rho(\vec{r}, t + dt) = \rho(\vec{r}, t) e^{-dt\vec{\nabla}\cdot\vec{v}} \tag{2.12}$$

From (Eqn. 2.7), it can be seen that the quantum effects are encapsulated into Q, which is a function of the curvature of the amplitude [12, 5]. Thus, quantum theory is connected to the corresponding classical picture via Q, the essence of Bohm's [8, 9] hydrodynamic formulation.

The mathematical equations describe the relations among the physical variables. Accurate representation of the initial and boundary conditions guided by the physical phenomena under investigation is thus, necessary for computational accuracy. Since propagation of the velocity (Eqn. 2.9) and density (Eqn. 2.12) field equations coupled through Q, is equivalent to solving the TDSE (Eqn. 1.1), appropriate initialization of these fields would be necessary for computational accuracy.

2.2 Quantum Trajectory Method

In this method, a collection of N quantum sub-particles (also referred to as 'pseudoparticles' or fluid mass points), each of mass m, is used to represent a physical particle with each pseudoparticle executing a "classical trajectory" governed by the Lagrangian QFD-EOM [12] and the quantum potential Q. (Eqn. 2.8). A mean behavior of all these "classical trajectories" trace a "quantum trajectory". Thus, this method is fully quantum mechanical and is distinct from classical or semi classical methods although it employs classical trajectories. Derivatives of ρ, v, and Q in the Lagrangian QFD-EOM are obtained by surface-fitting the corresponding component vectors of the pseudoparticles using the MLS

algorithm described in the next section. A weight factor is associated with each pseudoparticle depending on its location. Thus, the method is more appropriately called the moving weighted least squares (MWLS) algorithm. Since MWLS is a special case of MLS algorithm, in the present work the acronym MLS is used though the actual implementation is based on the MWLS approach.

2.3 MLS Algorithm

The moving least squares approximation (MLS), also known as the "meshless" method, is one of a class of recently developed methods. These methods are useful for spatial discretization [19, 20].

In MLS method, a function $f(x)$, in one-dimension, is assumed to have been defined on an unstructured set of points (or pseudoparticle positions) $\{x_i\}$ where, i=1,..,N_p (N_p is the number of pseudoparticles in the set). Note that $N_p \leq N$ where, N is the total number of pseudoparticles. The objective of the MLS method is to find an approximate value of f in the neighborhood of each $\{x_i\}$. A set of polynomials $\{p_j\}$ with j=1..N_b (where N_b is the number of basis states) were defined using a standard basis

$$p_j(x) = \frac{x^{(j-1)}}{(j-1)!} \tag{2.13}$$

such that

$$f_i(x) = \sum_{j=1}^{N_b} a_j p_j(x - x_i), \tag{2.14}$$

then, to determine the coefficients $\{a_j\}$, the approximation in (Eqn. 2.14) is constrained to pass through N_p, the size of the stencil, points in the neighborhood of x_i.

$$f_i(x_k) = \sum_{j=1}^{N_b} a_j p_j(x_k - x_i); \quad k = 1, 2, \ldots, N_p. \tag{2.15}$$

These equations are solved as an over-determined ($N_p > N_b$) linear least squares problem using a weight factor $w(x_{kl})$. The system of linear equations is solved using LU decomposition. Solving the linear system to minimize the error for $\{a_j\}$ leads to an equation for the solution vector $\vec{a}$ (of dimension $N_b \times 1$) in terms of the known function vector $\vec{f}$ (of dimension $N_p \times 1$). Thus, the derivatives of f can be expressed in terms of the known function values for the points in the stencil [12].

2.3.1 Pseudocode

Let $\{p_1, \cdots, p_n\}$ be the pseudoparticles, $\{x_1, \cdots, x_n\}$ be their positions and, $\{f_1, \cdots, f_n\}$ are the function values corresponding to the set $\{p_1, \cdots, p_n\}$. of pseudoparticles. Here, n $\leq$ N, the total number of pseudoparticles. Flow of the MLS algorithm is shown in Fig. 2.1.

2.4 Numerical Approach

This section provides the development of numerical formulas based on the differential form of the governing equations. Current computational methods for simulating wave-packet dynamics use space-time grids, basis sets, or some combination of both. Present study employed a uniform spatial grid in one-dimension. For the sake of completeness first, let us list the field equations and their correspondence with physical variables followed by discretized forms.

2.4.1 Governing Equations

Re-arranging the terms in the governing equations derived in the previous section we get the following equations

$$\rho(\vec{r}, t+dt) = \rho(\vec{r}, t)e^{-dt(\nabla\cdot\vec{v})} \quad \text{density,} \tag{2.16}$$

$$v(\vec{r}, t+dt) = \frac{-\nabla(Q+V)}{m}dt \quad \text{velocity,} \tag{2.17}$$

$$\vec{r}(t+dt) = \vec{r}(t) + \vec{v}dt \quad \text{position,} \tag{2.18}$$

$$f_q = -\nabla Q \quad \text{quantum force and,} \tag{2.19}$$

$$f_c = -\nabla V \quad \text{classical force} \tag{2.20}$$

2.4.2 Discretization Method

A fully explicit scheme is employed to update the field vectors. Since the present work is based on one-dimensional QTM with wave-packet propagating along the positive x-direction, discretized form of the governing equations are presented for one-dimension (along x-direction) and, generalization to two- and three-dimensions should be straightforward. Governing equations in discretized form are as under:

$$\rho_j^{n+1} = \rho_j^n e^{-\Delta t(\frac{\partial v}{\partial x})} \quad \text{density,} \tag{2.21}$$

$$v_j^{n+1} = v_j^n - \frac{\partial(Q+V)}{\partial x}\Delta t \quad \text{velocity,} \tag{2.22}$$

$$x_j^{n+1} = x_j^n + v_j^n\Delta t \quad \text{position,} \tag{2.23}$$

$$f_q = -\frac{\partial Q}{\partial x} \quad \text{quantum force and,} \tag{2.24}$$

$$f_c = -\frac{\partial V}{\partial x} \quad \text{classical force} \tag{2.25}$$

In the present study, for a free particle, the classical potential V=0 and force f_c=0. All the remaining spatial derivatives are computed using the MLS algorithm

while, the temporal derivatives are approximated using a forward differencing scheme. All pseudoparticles are uniformly distributed to provide a uniform grid for spatial distribution.

2.5 Shared-memory Model

Brook et al. [13] parallelized Lopreore and Wyatt's [12] MLS algorithm on an a shared-memory parallel computer using OpenMP directives. A high level description of the algorithm to track the state of the system is given in Fig. 2.2. In this algorithm, Let x[],v[], and ρ[] denote the arrays of values of the positions, velocities, and probability densities respectively, of N pseudoparticles in the wave-packet representing the physical particle. These arrays are initialized before the first simulation step. During each time step, values for the classical potential cV[], and classical force cF[] are computed for each pseudoparticle. In this model, the main computational loop running over the pseudoparticles contains several sub-loops that perform desired calculation.

In the MLS algorithm, each pseudoparticle sorts its nearest neighbors based on a parametric value that determines the neighborhood to form the set $\{x_i\}$ where i=1,..,n. Their corresponding $\{f_i\}$ will be used to compute the coefficients $\{a_j\}$ using (Eqn. 2.15). Thus, each pseudoparticle has its own set of $\{x_i\}$ and $\{f_i\}$. This set is to be formulated in every time step of the simulation. For computing the derivatives of ρ (for computing Q), v (for computing ρ), and Q (for computing quantum force), an MLS call will be issued for each of the pseudoparticles. Since MLS routine requires information from the other members of its set $\{x_i\}$ and $\{f_i\}$ for surface fitting, a barrier synchronization would be necessary. There are four barrier synchronization calls (three MLS calls plus one main loop for thread synchronization) in the OpenMP implementation. In this algorithm, an implicit

Do for each pseudoparticle in turn:

1. **Sort pseudoparticles with respect to p_i Set up the $n \times m$ polynomial basis matrix P**

$$P(i,j) = \begin{bmatrix} 1 & x_1 & {x_1}^2 & \cdots & {x_1}^n \\ 1 & x_2 & {x_2}^2 & \cdots & {x_2}^n \\ \vdots & \vdots & \vdots & \ddots & \vdots \\ 1 & x_m & {x_m}^2 & \cdots & {x_m}^n \end{bmatrix}$$

2. **Let W be the $n \times n$ diagonal weight matrix such that $W(i,i) = w_i$ for $i = 1, ..., n$. Now set up the $m \times m$ matrix $A = P^T W P$**

$$A(i,j) = \begin{bmatrix} w_1 & w_2 & w_3 & \cdots & w_n \\ w_1x_1 & w_2x_2 & w_3x_3 & \cdots & w_nx_n \\ w_1{x_1}^2 & w_2{x_2}^2 & w_3{x_3}^2 & \cdots & w_n{x_n}^2 \\ \vdots & \vdots & \vdots & \ddots & \vdots \\ w_1{x_1}^n & w_2{x_2}^n & w_3{x_3}^n & w_4{x_4}^n & w_n{x_n}^n \end{bmatrix} \begin{bmatrix} 1 & x_1 & {x_1}^2 & \cdots & {x_1}^m \\ 1 & x_2 & {x_2}^2 & \cdots & {x_2}^m \\ 1 & x_3 & {x_3}^2 & \cdots & {x_3}^m \\ \vdots & \vdots & \vdots & \ddots & \vdots \\ 1 & x_n & {x_n}^2 & \cdots & {x_n}^m \end{bmatrix}$$

3. Now set up a $m \times 1$ matrix $R = P^T W f$

$$R(i,j) = \begin{bmatrix} w_1 & w_2 & w_3 & \cdots & w_n \\ w_1x_1 & w_2x_2 & w_3x_3 & \cdots & w_nx_n \\ w_1{x_1}^2 & w_2{x_2}^2 & w_3{x_3}^2 & \cdots & w_n{x_n}^2 \\ \vdots & \vdots & \vdots & \ddots & \vdots \\ w_1{x_1}^m & w_2{x_2}^m & w_3{x_3}^m & \cdots & w_n{x_n}^m \end{bmatrix} \begin{bmatrix} f_1 \\ f_2 \\ f_3 \\ \vdots \\ f_n \end{bmatrix}$$

4. **Solve the linear system $Ax = R$ which is equivalent to solving $Px = f$ to obtain the coefficients $\{a_j\}$ that "best fits" the polynomial** where, $x = \{x_1, x_2, .., x_n\}^T$

Figure 2.1: Moving Least Squares Approximation Algorithm

method is employed for computing the density, and velocity of each pseudoparticle, and an explicit scheme is used for computing all other terms.

```
Initialize x[ ], v[ ], ρ[ ]
    for each time step do
        for pseudoparticle i = 1 to N do
            Call MLS (i, x[ ], ρ[ ])
            Compute quantum potential qV[i]
        end for
        for pseudoparticle i = 1 to N do
            Call MLS (i, x[ ], qV[ ])
            Compute quantum force qF[i]
        end for
        for pseudoparticle i = 1 to N do
            Compute classical potential cV[i], force cF[i]
            for pseudoparticle i = 1 to N do
                Update position using velocity from previous time step
                Update velocity using classical and quantum forces computed
                in this time step
            end for
            for pseudoparticle i = 1 to N do
                Call MLS (i, x[ ], v[ ])
                Compute gradient of velocity dv[i] using velocities
                just computed
            end for
            for pseudoparticle i = 1 to N do
                Update density using the divergence of the velocity
                field just computed
            end for
            Output time, x[ ], v[ ], ρ[ ], cV[ ], cF[ ], qV[ ], qF[ ], dv[ ]
        end for
    end for
```

Figure 2.2: Algorithm for QTM using MLS on OpenMP

CHAPTER III

IMPLEMENTATION

3.1 Velocity Distribution

With group velocity approximation, a wave-packet centered around some k_0 accurately represents a particle moving with a velocity v_0. Thus, appropriate choice of $\Delta k = |k - k_0|$ such that, the wave-packet is narrowly peaked around k_0 is the key for accuracy in this representation. With N pseudoparticles distributed in coordinate space representing the wave-packet in QTM, choice of Δk implies distribution of velocities among these pseudoparticles. In the previous work by Brook et al [13], all pseudoparticles in momentum space were initialized with the particle velocity v_0. That is, they chose Δk=0 in their accuracy study.

It is well known that a wave-packet moving with a velocity spreads (relative separation of trajectories with time) non-uniformly and a wave-packet at rest spreads uniformly. It is also known that the rate of spreading is proportional to β, the width of the initial Gaussian wave-packet for t>0, and it corresponds to the spread Δk in the momentum space via the uncertainty principle. Since the $\hat{p}$ operator commutes with $\hat{H}$ and $\hat{p}$ is independent of time for a free particle moving with constant velocity, the width Δk of the wave-packet in momentum space chosen at t=0 is preserved at all times. Thus, appropriate choice of Δk that satisfies the group velocity assumption would be necessary to accurately represent a free particle via wave-packet methods.

For a chosen Δt, the evolution of the probability density (Eqn. 2.16) is mostly dependent on the gradient of the velocity. And the velocity update (Eqn. 2.17)

depends on the probability density via the quantum force (hence, the quantum potential). In the absence of classical force, for a free particle, the velocity update (Eqn. 2.17) is slow, especially when m is large. The velocity of each pseudoparticle is further used to update its position after each time step Δt. Since the probability density field is initialized directly from the state function, and the validity of the MLS algorithm in approximating the dynamics has been amply demonstrated, the *transient effect* is mainly a result of inappropriate initialization of pseudoparticle velocities. Hence, remaining part of this section is devoted for deriving velocity distribution among pseudoparticles.

In the accuracy studies of Brook et al. [13, 21], a free particle is represented by a Gaussian wave-packet (GWP) with center k_0 and width β given by

$$\Psi = \left(\frac{2\beta}{\pi}\right)^{\frac{1}{4}} \exp(-\beta(x - x_0)^2 + ik_0x), \tag{3.1}$$

where $k_0 = 10.45715361$, $\beta = 10$ and $x_0 = 2$. Here, x_0 is the center of the wave-packet.

Fourier transform of the initial GWP (Eqn. 3.1) in position space is employed to obtain the corresponding momentum distribution function $\phi(k)$. Squared modulus of $\phi(k)$ is obtained using the equation

$$\phi(k)^*\phi(k) = \left[\left(\frac{2\beta}{\pi}\right)^{1/4}\left(\frac{\pi}{\beta}\right)^{1/2} e^{-\frac{1}{4\beta}(k-k_0)^2}\right]^2 \tag{3.2}$$

Using the normalization condition

$$\int_{-\infty}^{+\infty} |\phi(k)|^2 = 1 \tag{3.3}$$

to compute the normalization factor, one obtains squared modulus of the normalized momentum distribution function $|\phi(k)|^2$. Using this function and its parametric width Δk, pseudoparticle velocities can be derived by distributing them in the interval $\left[|\phi(k)|^2 - \Delta k, |\phi(k)|^2 + \Delta k\right]$ and using pseudoparticle mass m=2000 a.u.

3.2 Message Passing Interface

In distributed memory computing, contrary to the shared-memory model, most of the overhead is a result of explicit communication calls between the processing elements. Implicit update of the velocity and density fields is a source of communication overhead in distributed memory computing environment.

3.2.1 Fully Explicit Method

The present study employed a fully explicit algorithm for propagating the wave-packet. In this method, the computational interdependencies are reduced by enforcing that all the terms in the current time step depend only on the previous time step. This approach enables efficient problem distribution among available processors. Since the QFD formalism is casted into an IVP via the density and velocity field equations, the accuracy of the method is more sensitive to field initialization compared to propagation. Thus, the difference between fully explicit and partially implicit update is not expected to produce an accountable error.

3.2.2 Pseudocode

A high level description of the algorithm to track the state of the system is given in Fig. 3.1. The algorithm implements fully explicit update for all component

vectors of each of the pseudoparticle. All of the **for** loops are parallel loops. The iterates could be performed in any order and further, the iterates of a loop perform the same computations.

From Fig. 3.1, it is clear that large part of the computational overhead is mainly due to the MLS calls. Since the MPI version also employs the same MLS algorithm that is used by Brook et al. [13], barrier synchronizations would still be necessary in the current implementation.

One way to reduce barrier synchronizations is through further reducing computational interdependencies. This could be accomplished, particularly with the fully explicit method, by replicating the data arrays on all processors. Since the MLS routine contributes largely to the computational overhead, its parallelization is expected to improve the speedup significantly.

By reorganizing the updates, and computations, number of synchronizations required has been reduced to two in the current implementation. The first synchronization is needed after the computation of qV[ ] to make the results available to all processors for computation of qF[ ] and the second one required to gather the results of the computations of qF[ ] and dv[ ]. From timing experiments using N=2001 for the one-dimensional harmonic oscillator problem, a speedup of about 26.4 with an efficiency of about 82% were obtained using 32 processors. Further details on the implementation and performance analysis can be found in Cariño et al. [22].

Initialize $x[\ ]$, $v[\ ]$, $\rho[\ ]$
for each time step **do**
  for pseudoparticle $i = 1$ to N **do**
    Call MLS $(i, x[\ ], \rho[\ ])$
    Compute quantum potential $qV[i]$
  end for
  for pseudoparticle $i = 1$ to N **do**
    Call MLS $(i, x[\ ], qV[\ ])$
    Compute quantum force $qF[i]$
  end for
  for pseudoparticle $i = 1$ to N **do**
    Call MLS $(i, x[\ ], v[\ ])$ Compute gradient of velocity $dv[i]$
  end for
  for pseudoparticle $i = 1$ to N **do**
    Compute classical potential $cV[i]$, force $cF[i]$
  end for
  Output time, $x[\ ], v[\ ], \rho[\ ], cV[\ ], cF[\ ], qV[\ ], qF[\ ], dv[\ ]$
  for pseudoparticle $i = 1$ to N **do**
    Update density $\rho[i]$
  end for
  for pseudoparticle $i = 1$ to N **do**
    Update position $x[i]$ and velocity $v[i]$
  end for
end for

Figure 3.1: Algorithm for QTM using MLS on MPI

CHAPTER IV

ACCURACY STUDY

4.1 Initialization

All the pseudoparticles are uniformly distributed around x_0 in order to represent a physical particle of size 2.0 a.u. such that the spatial resolution Δx is given by $2.0/N$. Each pseudoparticle is initialized with velocity computed from $|\phi(k)|^2$ and a parametric choice of Δk that satisfies the group velocity assumption, and its probability density is set to the square of the modulus of the state function at each position. The wave-packet is then propagated for a specified number of time steps using a step size Δt.

4.2 Numerical Experiments

With approximately symmetric $\phi(k)$ around k_0, accuracy of the computed solution a for non-uniformly spreading wave-packet could be conceived by appropriate choice of Δt. Thus, appropriate choice of Δk that satisfies group velocity assumption, and Δt for wave-packet propagation would be necessary for computational accuracy.

With this view, the numerical experiments of Brook et al. [13, 21] were repeated with Δk from the set $\{0, 0.001, 0.005, 0.01\}$ and Δt from the set $\{0.0625, 0.125, 0.25, 0.5\}$ and the number of pseudoparticles from the set $\{21, 51, 81, 111, 141\}$. For all these experiments six basis functions were used to construct the polynomials in the MLS algorithm. All pseudoparticles formed the stencil for computing the derivative of the quantum potential Q while, half of them were used

for computing the derivatives of velocity and density. Further details on these choice considerations are available in Brook et al. [13]. The spatial resolution was fixed at $\Delta x = 0.095$, corresponding to N=21. This choice was based on the observation, from Figure 1.2, that the relative error for N=21 set an upper bound and the impact of choosing the (Δk, Δt) pair would be significant.

CHAPTER V

RESULTS AND DISCUSSION

The influence of initializing the pseudoparticle velocities, by parametric choice of Δk, on the *transient effect* for a fixed Δt=0.0625 is demonstrated in Figure 5.1. It can be seen from this figure that, the *transient effect* completely vanishes with $\Delta k = 0.005$ as the parameter for the initial velocity distribution compared with $\Delta k = 0$ for which the initial pseudoparticle velocities are set to the particle velocity. However, the maximum error is almost double with $\Delta k = 0.005$ compared to that with $\Delta k = 0$.

It is well known that nearly monotonic variation of both the probability density and phase[1] density are the essential ingredients of the QFD formulation. Onset of the *transient effect* during the boost phase with $\Delta k = 0$ contradicts this vital aspect. For a given $\Psi(x, 0)$ representing a particle moving with a velocity, there exists a Δk in momentum space that accurately represents the particle velocity. That is, inappropriate choice of Δk (hence, inappropriate velocity field initialization) contributes to error in computing the particle velocity as well as the particle position. Since the density update (Eqn. 2.12) depends on the velocity gradient, the *transient effect* resulting from improper velocity field initialization (via inappropriate choice of Δk) could be responsible for the apparent accuracy with $\Delta k = 0$.

[1]The phase effects are cancelled out in the present study with choice of probability density $|\Psi^*\Psi|$ for the accuracy study.

The behavior of the gradient of the velocity of each pseudoparticle with $\Delta k = 0$ and $\Delta k = 0.005$, for fixed Δt=0.0625, are illustrated in Figs 5.2 and 5.3, respectively. The time region of interest is the range 30–110 a.u., at which the *transient effect* is manifested.

In Fig. 5.2 where Δk=0, the gradient of velocity continues to increase with a positive slope. This means, in order to maintain nearly monotonic behavior of probability density, sufficiently small Δt has to be chosen to compensate for the growth in velocity gradient in the density update equation (Eqn. 2.12). The *transient effect* thus is more sensitive to Δt, which is in conformity with dependence of the amplitude of the *transient effect* on Δt shown in Fig. 1.3.

In Fig. 5.3, where Δk=0.005, the increase in gradient of velocity saturates during the peak region (t=70-80 a.u. of propagation) of the *transient effect*. From then on, the slope is invariant; thus, the corresponding density update is nearly monotonic as required by the QFD formalism.

The accuracy of probability density with fixed Δk=0.005 and Δt chosen from the set {1, 0.25, 0.0625} is shown in Fig. 5.4. From this figure, it is evident that Δt=0.0625 offers the best accuracy. Experiments with fixed Δt=0.0625 and varied Δk from the set {0, 0.001, 0.005, 0.01}, shown in Fig. 5.5, confirm this observation.

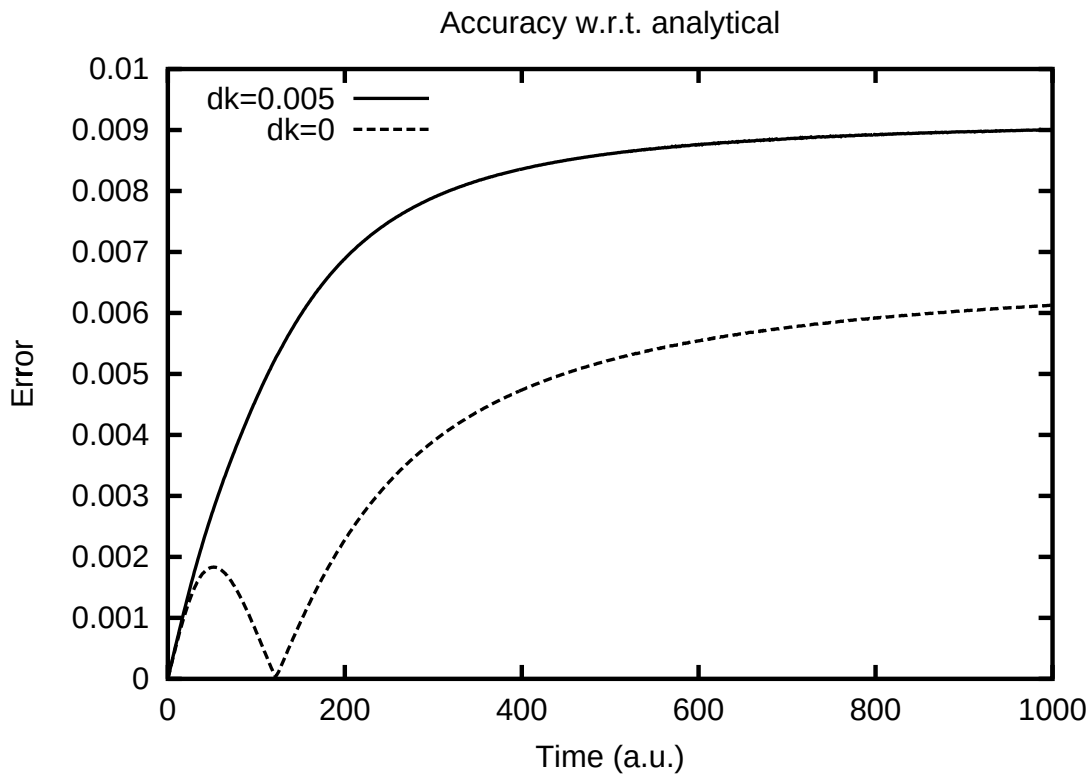

Figure 5.1: Dependence of the *transient effect* on Δk with Δt=0.0625

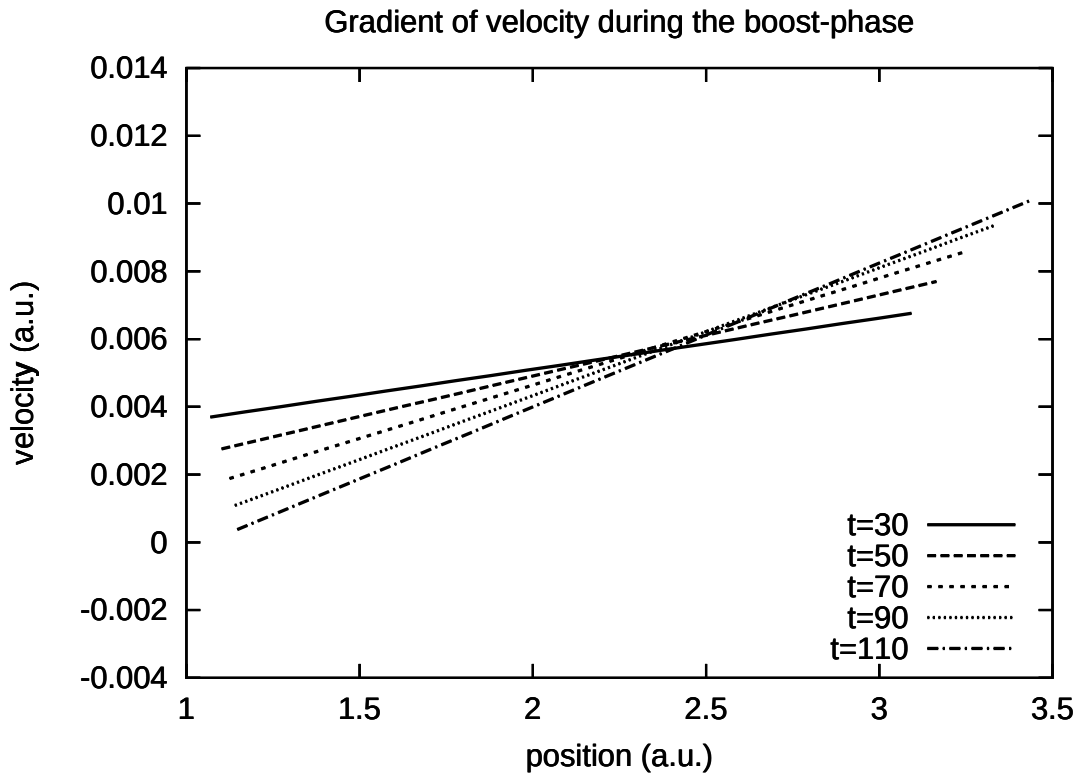

Figure 5.2: Gradient of velocity during the transient region with $\Delta k = 0$ and Δt=0.0625

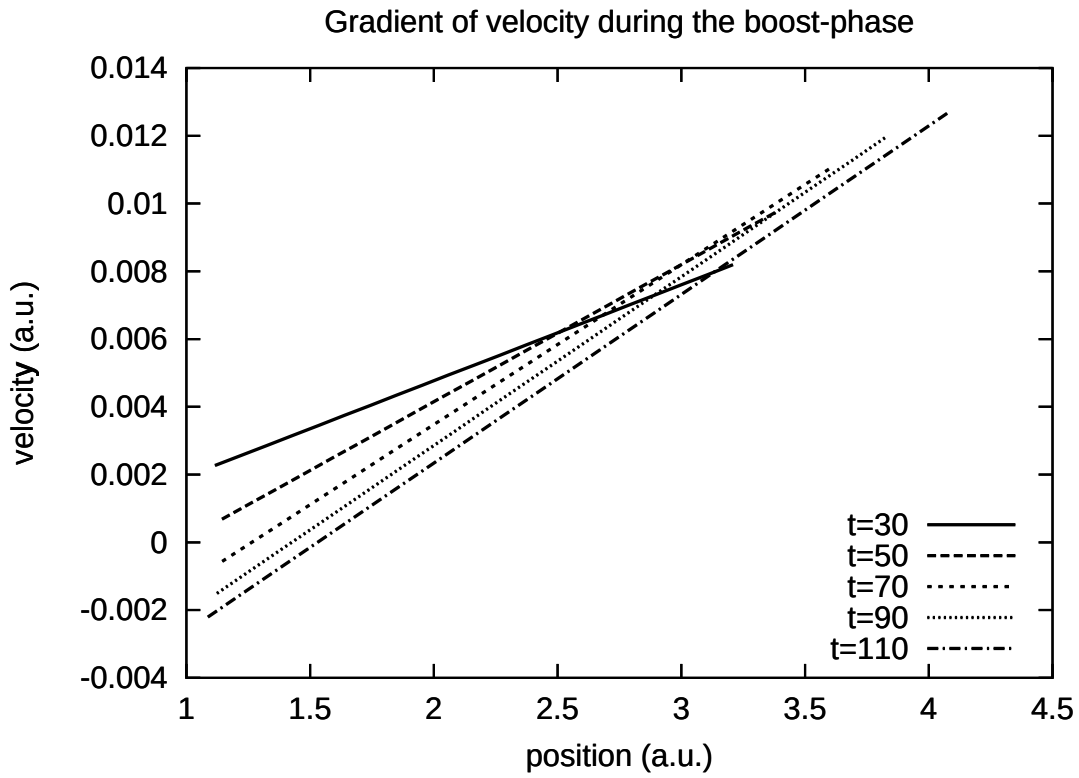

Figure 5.3: Gradient of velocity during the transient region with $\Delta k = 0.005$ and Δt=0.0625

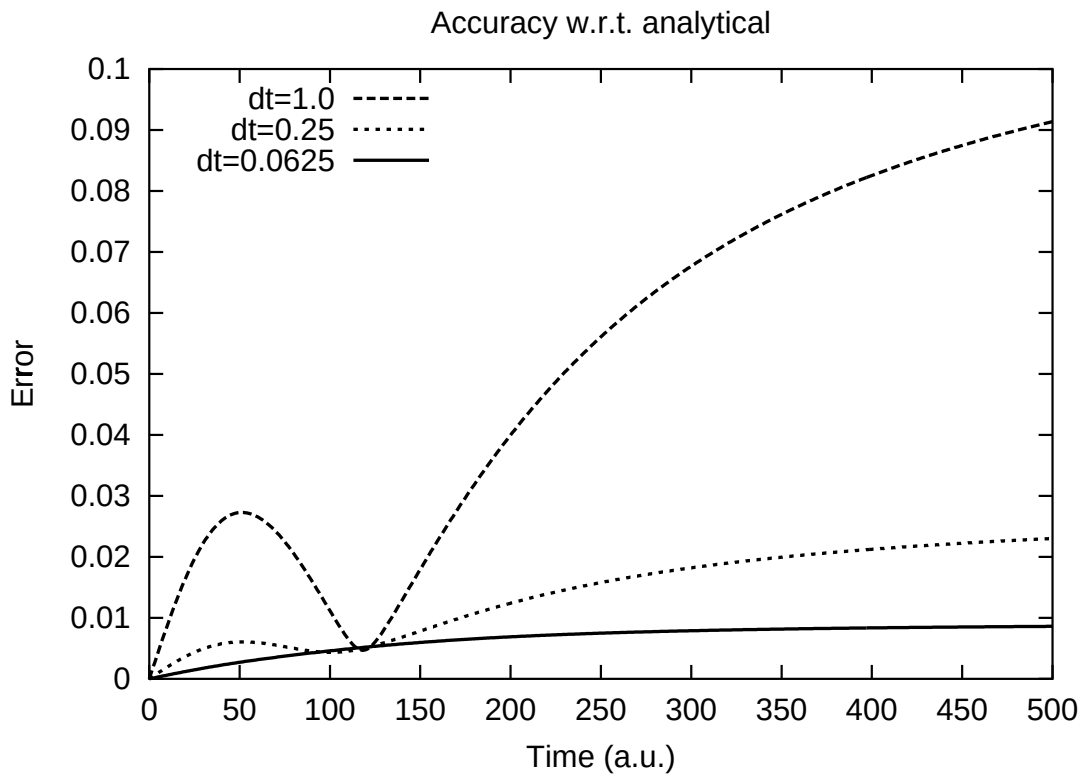

Figure 5.4: Dependence of accuracy on time step size with Δk=0.005

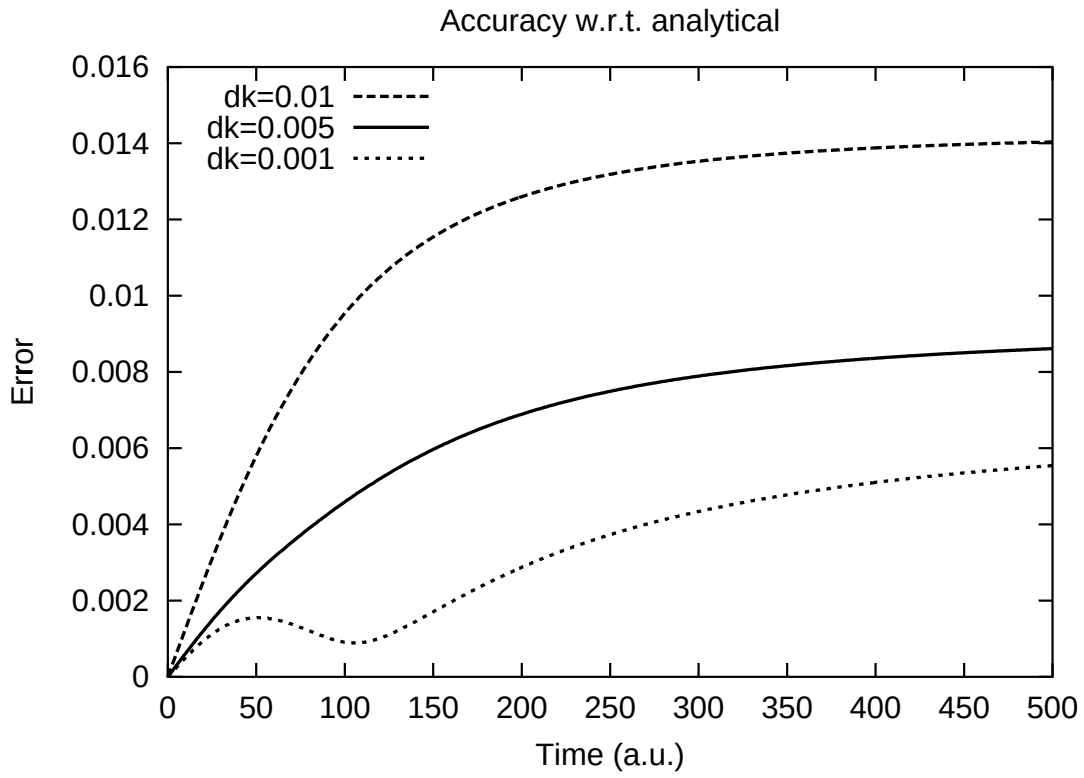

Figure 5.5: Dependence of accuracy on the initial velocity spread with Δt=0.0625

CHAPTER VI

SUMMARY AND CONCLUSIONS

Quantum Fluid Dynamics replaces solving the time-dependent Schrödinger equation by a density and velocity field equations coupled through the quantum potential Q, which is inherently global in nature. In this formalism, a quantum mechanical system is represented by a compressible and irrotational fluid of density (ρ) and of mass m moving with an average velocity (v). In this formalism, the amplitude and phase of the system wavefunction Ψ are nearly monotonic functions of time. With close parallelism of the QFD with CFD, Bohm's hydrodynamic formalism connects quantum dynamics with its classical counterparts through Hamilton-Jacobi theory. In this approach, the "quantum potential" (Q) encapsulates all the quantum mechanical effects. Thus, Bohmian dynamics offers a formalism to move a step closer to unify the nondeterministic (quantum) and deterministic (classical) theories of matter.

The Quantum Trajectory Method is derived from Bohm's hydrodynamic formalism. In this method, a collection of N pseudoparticles (or quantum subparticles) represent the system wavefunction and each pseudoparticle executes a "classical trajectory" governed by the QFD-equations of motion and Q. These trajectories span the propagation of the wave-packet. The characteristic vectors of the fluid, namely ρ, v, and Q, are obtained by surface-fitting the pseudoparticles using an MLS algorithm.

The Quantum Trajectory Method, although utilizing classical trajectories, is a fully quantum mechanical model, which is distinct from classical or semi-

classical paradigms. The QTM provides an excellent model for simulating quantum dynamics on parallel and distributed computing environments. The present study sets another example for this observation.

The Quantum Trajectory Method is implemented on distributed memory computing environment using MPI communication libraries, with fully explicit method for updating the wave-packet. This implementation has reduced the number of barrier synchronizations to two from four with OpenMP implementation by Brook et al.

From the present study, computational accuracy of QTM for a free particle depends on appropriate initialization of both the density and velocity fields. For a free particle, with the probability density of each pseudoparticle computed directly from the state function, the onset of the *transient effect* is a result of inappropriate initialization of the velocity field. More appropriate pseudoparticle velocities were assigned using $|\phi(k)|^2$, the normalized squared modulus of the initial momentum distribution function, and parametric choice of the width Δk. $\phi(k)$ was obtained by the Fourier transform of the initial Gaussian wave-packet for a free particle.

Numerical experiments with parametric choice of Δk from the set $\{0,\ 0.001,\ 0.005,\ 0.01\}$, and Δt from the set $\{0.0625,\ 0.125,\ 0.25,\ 0.5\}$ for N=21 reveal that the onset of the *transient effect* is sensitive to initialization of the velocity field (hence, choice of Δk), and its amplitude depends on Δt. These experiments also suggest that $\Delta k = 0.005$ and $\Delta t = 0.0625$ offer the best accuracy for the probability density while, satisfying nearly monotonic behavior (an essential ingredient of the QFD formulation).

A thorough investigation of the interdependency of Δk and Δt that amounts to computing the rate of spreading could be a useful guide for more accurate choice

of Δk. Since the effect of the choice of Δk looses much of its significance in the presence of a classical force, the current work is confined to a parametric study.

CHAPTER VII

FUTURE WORK

The present study does not validate the nearly monotonic nature of the real valued phase function S with respect to size of the time step. This is mainly because of the cancelation of phase effects with the computation of probability density. A method to compute the probability density directly from R, the real part of the wavefunction, would be helpful in retaining S (the imaginary part of the wavefunction) and thus, the phase effects from cancelling out. These phase effects are expected to provide significant insight to the stability analysis of the QTM. Since the gradient of S is useful for assigning pseudoparticle velocities, this effort may also improve the accuracy of the probability density. Hence, resolving these issues would be the immediate future interest.

It is well known that one-dimensional methods are good for model problems. Any realistic application needs at least a 2D and preferably 3D implementation. Hence, these options will be explored in continuation of the present work. Also, the present study employed a uniform computational grid with fixed time step size throughout the simulation. However, adaptive temporal and spatial resolutions would be more appropriate for efficient simulations especially in the presence of time varying fields. Since implicit methods have much to offer for both stability and accuracy with adaptive time stepping, investigation of these aspects formed an essential component of the future work.

It is clear that the MLS method is largely contributing to computational overhead in the present one-dimensional implementation of the QTM. In 2D, and

3D QTM, one has to deal with mixed and higher order derivatives as well. Hence, efficient parallelization of the MLS method might be necessary. Exploring the applicability of parallel math libraries such as BLAS and LAPACK for solving the system of equations in the MLS method would be resourceful. Hence, this effort would form an important component for extending the QTM into higher dimensions.

It would also be of tremendous interest to investigate the accuracy of the Quantum Trajectory Method for multi-particle correlations (at least two particles to start with) in the presence of time-dependent potentials. This effort, though not straightforward, has significant impact on validating the applicability of Bohm's hydrodynamic formalism for research in Quantum Computing (QC) and Quantum Information Processing (QIP).

REFERENCES

[1] A. J. and M. Saltzer, "Semiclassical wave packet tunneling in real-time," *Phys. Lett. A*, 2002.

[2] S. Rolston and W. D. Phillips, "Nonlinear and quantum atom optics," *Nature*, vol. 416, p. 219, 2002.

[3] L. De Broglie *C R Acad. Sci. Paris*, vol. 183, p. 447, 1926.

[4] L. De Broglie *C R Acad. Sci. Paris*, vol. 184, p. 273, 1927.

[5] P. E. Holland, *The Quantum Theory of Motion:An account of the de Broglie-Bohm Causal Interpretation of Quantum Mechanics.* Cambridge University Press, 1993.

[6] E. Madelung *Z Phys.*, vol. 40, p. 322, 1927.

[7] M. L. Goldberger and K. M. Watson, *Collsion Theory.* Wiley: New York, 1964.

[8] D. Bohm, "A suggested interpretation of the quantum theory in terms of "hidden" variables .i," *Phys. Rev.*, vol. 85, p. 166, 1952.

[9] D. Bohm, "A suggested interpretation of the quantum theory in terms of "hidden" variables .ii," *Phys. Rev.*, vol. 85, p. 180, 1952.

[10] E. Wigner, "On the quantum correction for thermodynamic equilibrium," *Phys. Rev.*, vol. 40, p. 749, 1932.

[11] E. F. Toro, *Riemann Solvers and Numerical Methods for Fluid Dynamics.* Springer-Verlag, 1999.

[12] C. L. Lopreore and R. E. Wyatt, "Quantum wave packet dynamics with trajectories," *Phys. Rev. Lett.*, vol. 82, p. 5190, 1999.

[13] R. G. Brook *et al.*, "Solving the hydrodynamic formulation of quantum mechanics:a parallel mls method," *Int. J. of Quant. Chem.*, vol. 85, p. 263, 2001.

[14] A. Bamazi and B. M. Deb, "The role of single-particle density in chemistry," *Rev. Mod. Phys.*, vol. 53, p. 95, 1981.

[15] A. Bamazi and B. M. Deb, "The role of single-particle density in chemistry," *Rev. Mod. Phys.*, vol. 53, p. 593, 1981.

[16] B. Deb and P. K. Chattaraj, "New quadratic nondifferential thomas-fermi-dirac type equation for atoms," *Phys. Rev. A*, vol. 37, p. 4030, 1988.

[17] A. M. Meirmanov *et al.*, *Evolution Equations and Lagrangian Coordinates.* Walter de Gruyter: New York, 1997.

[18] F. Mayer *et al.*, "Quantum fluid dynamics in the lagrangian representation and applications to photodissociation problems," *J. Chem. Phys.*, vol. 111, p. 2423, 1999.

[19] T. Belytschko *et al. Comput. Methods Appl. Mech. Eng.*, vol. 139, p. 3, 1996.

[20] T. J. Liszka *et al.*, "hp-meshless cloud method," *Comput. Meth. Appl. Mech. Eng.*, vol. 139, p. 263, 1996.

[21] R. Brook *et al.*, "Accuracy studies of a parallel algorithm for solving the hydrodynamic formulation of the time-dependent schrödinger equation," *J. Molecu. Struct.(Theochem)*, vol. 592, p. 69, 2002.

[22] R. Cariño *et al.*, "Wavepacket dynamcis using the quantum trajectory method on message-passing systems," in *Proceedings of the ITAMP Workshop on Computational Approaches to time-dependent quantum dynamics, May 9-11, Harvard Univeristy, MA*, 2002.